Finite-size effects at 2D Ising critical points via conformal mapping

1986 J. Phys. A: Math. Gen. 19 437

(http://iopscience.iop.org/0305-4470/19/3/024)

J. Phys. A: Math. Gen. 19 (1986) 437-451. Printed in Great Britain

Finite-size effects at 2D Ising critical points via conformal mapping

P Kleban†‡§, G Akinci‖‡, R Hentschke¶§ and K R Brownstein¶

† Laboratory for Surface Science and Technology and Department of Physics, University of Maine at Orono, Orono, ME 04469, USA
‖ Turktelefon, Izmir, Turkey
¶ Department of Physics, University of Maine at Orono, Orono, ME 04469, USA

Received 18 February 1985, in final form 14 June 1985

Abstract. Using recent results by Cardy based on conformal invariance of critical correlation functions we calculate universal results for scattering functions $S(k)$, susceptibilities, correlation lengths and specific heat correction terms for finite Ising systems in two dimensions with circular, elliptical and rectangular shapes and free boundary conditions. Our results show the effects of critical order on these quantities. For a circle, $S(k)$ decays as $1/k^{2-\eta_{app}}$ for a large range of intermediate k values with an 'apparent' exponent $\eta_{app} = 0.09$. The probable influence of end, edge and domain wall effects in the rectangular geometry is discussed. Application of our results to experimental systems and other theoretical models is discussed.

1. Introduction

Recent work by Cardy (1984a, b) on the conformal invariance of critical *correlation functions* greatly extends the theory (Barber 1983, Kleban 1984) of finite-size effects at critical points since most previous results applied to thermodynamic quantities. In this paper we apply Cardy's results to the numerical determination of (elastic) scattering functions $S(k)$, bulk susceptibilities, correlation lengths and specific heat correction terms for finite two-dimensional systems. We consider circular, square and rectangular shapes for 2D Ising systems with free boundaries. Some calculations for elliptical shapes are also mentioned. Our results are universal for each shape considered. They specify the effects of shape and critical order on the quantities considered. This complements previous work on shape effects on the free energy, energy and specific heat for the simple Ising model with periodic boundary conditions and rectangular geometries in the critical region (Ferdinand and Fisher 1969, Kleban and Akinci 1983a, b) and scattering functions for infinite systems (Tracy and McCoy 1975 and references therein).

In § 2 we review some general features of the conformal theory. Application to the circular geometry is made, and a universal vanishing of any correlation function demonstrated. Section 3 defines the scattering function $S(k)$, susceptibility and specific heat correction term and gives results for these quantities in a circular region. An interesting power-law behaviour of $S(k)$ is shown and discussed. Results for rectangular

‡ Supported in part by NATO Research Grant No 088/84.
§ Supported in part by the US Office of Naval Research.

regions are presented in § 4. The dependence of the various quantities on aspect ratio s is shown. For the correlation length, susceptibility and specific heat, this is discussed in terms of the effects of a 1D Ising array of domain walls (Kleban and Akinci 1983a, b), end and edge effects. A few results for elliptical shapes are also mentioned.

Conformal invariance applies in the field theoretic limit, which means one is treating the critical point with a continuum theory. In this context, our results are exact, within numerical errors. Their application to lattice models or other systems generally involves corrections at short distances, e.g. when the wavevector $k \sim 1/a$, where a is a lattice spacing. This is discussed further in § 5. We also make some remarks on the connection of conformal results, which are valid *at* the critical point $T = T_c$ only, with what one expects in the critical region (T near T_c). Some additional comments on the application of our results to experimental and model systems are also included in § 5. Computational details are considered in § 6.

2. Conformal invariance—general features and circle map

Conformal invariance of critical correlation functions (Polyakov 1970, 1974, Wegner 1976) implies that local scalar operators ϕ at T_c satisfy

$$g(z_1, z_2) = \langle \phi(z_1)\phi(z_2)\rangle = |w_1'|^x |w_2'|^x \langle \phi(w_1)\phi(w_2)\rangle \tag{1}$$

where $z \to w(z)$ is an arbitrary conformal transformation, $w_i \equiv w(z_i)$, x is the critical dimension of the operator ϕ (e.g. $x = \frac{1}{8}$ for the 2D Ising spin operator) and z and w are ordinary complex numbers. Equation (1), which we have expressed in a form appropriate for two-dimensional systems, is valid quite generally (Cardy 1984b); however, the constraints it implies are strongest in two dimensions (Belavin *et al* 1984a, b, Dotsenko 1984a, b, Friedan *et al* 1984) since the conformal group is infinite dimensional. Note that equation (1) may be viewed as a generalisation of scale invariance, with $|w'|$ a position-dependent scale parameter.

Cardy (1984a) has exploited equation (1) in two dimensions by using a *finite* conformal transformation to map $g_z \equiv \langle \phi(z_1)\phi(z_2)\rangle$ in the plane into the corresponding $g_w \equiv \langle \phi(w_1)\phi(w_2)\rangle$ in a semi-infinite strip. In particular, this can be used to explain the form of the universal finite-size amplitude of the correlation length. In further work, Cardy (1984b) has employed the properties of *infinitesimal* conformal transformations to determine completely the functional form of the correlation function in the half-plane with free boundary conditions. This has been accomplished for the Ising model spin–spin and energy–energy correlation functions and some other cases. In this paper we use Cardy's latter results for Ising systems in the half-plane and equation (1) with finite conformal transformations to calculate various quantities of interest in finite systems by mapping the half-plane into elliptical and rectangular regions.

Before describing our specific results, we review some universal features of critical correlation functions in semi-infinite geometries with free boundaries (Cardy 1984b). Let $G(\boldsymbol{r}_1, \boldsymbol{r}_2) = \langle \phi(\boldsymbol{r}_1)\phi(\boldsymbol{r}_2)\rangle$ be a two-point function in arbitrary dimension, with $G = 0$ on the boundary surface, which we define by $y = 0$. Conformal invariance then implies that

$$G(r_1, r_2) = (y_1 y_2)^{-x} \Phi\{[(x_1 - x_2)^2 + y_1^2 + y_2^2]/y_1 y_2\} \tag{2}$$

where $\boldsymbol{x}$ is the part of $\boldsymbol{r}$ parallel to the bounding surface. In arbitrary dimension, the form of Φ is not determined by conformal invariance; however, other arguments fix

its asymptotic behaviour in certain limits. If y_1, $y_2 \to \infty$ with $|x_1 - x_2|$ fixed, the bulk limit is attained, and $G \sim |r_1 - r_2|^{-2x}$ implies

$$\Phi(2+\varepsilon) \to \varepsilon^{-x}, \qquad \varepsilon \to 0. \tag{3}$$

On the other hand, when $|x_1 - x_2| \to \infty$ with y_1, y_2 fixed, one expects (Binder 1983) surface critical behaviour with $G \sim |x_1 - x_2|^{-2x_s}$, where x_s is a surface critical exponent. This in turn implies

$$\Phi(\xi) \to \xi^{-x_s}, \qquad \xi \to \infty. \tag{4}$$

Similarly one can determine the form of G with one point near the surface and the other in the bulk. We will show below that equations (1) and (4) in fact imply a universal form for the vanishing of G at the edge of a finite circular region. In two dimensions, conformal invariance also determines the function Φ.

Now consider mapping the half-plane $y > 0$ (with free boundary conditions on the real axis) into a circle of radius one via the transformation

$$w = (z - \mathrm{i})/(z + \mathrm{i}). \tag{5}$$

This takes the point at infinity onto $w = 1$, and $z = 0$ onto $w = -1$, with the real axis in the z plane mapped onto the circumference of the circle. The correlation function $g(w_1, w_2)$ is determined via equation (1), with the Ising spin-spin correlation function in the half-plane given by equation (2) with $x = \frac{1}{8}$ and (Cardy 1984b)

$$\begin{aligned} &\Phi = 4^{-1/8}(\rho^{1/4} - \rho^{-1/4})^{1/2}, \\ &\rho \equiv |(x_1 - x_2)^2 + (y_1 + y_2)^2| / |(x_1 - x_2)^2 + (y_1 - y_2)^2|. \end{aligned} \tag{6}$$

The constant in equation (6) is chosen so that $g \to |r_{12}|^{-1/4}$ in the bulk limit.

Equation (5) maps the half-plane into the circle in a very non-uniform way, and one might well wonder whether $g(w_1, w_2)$ respects the symmetries of the circle. In fact, combining equations (2), (5) and (6) gives

$$\begin{aligned} g(w_1, w_2) &= \frac{1}{(1 - |w_1|^2)^x (1 - |w_2|^2)^x} \Phi(\xi), \\ \xi &= \frac{(1 - |w_1|^2)(1 - |w_2|^2)}{|w_1 - w_2|^2} + 1, \end{aligned} \tag{7}$$

so that the form given by equation (2) displays full circular symmetry. The correlation functions obtained for the elliptical and rectangular geometries considered below also exhibit the symmetries of these shapes. Similar symmetries for order-parameter profiles in finite systems with infinite-field boundary conditions have been demonstrated by Burkhardt and Eisenriegler (1985). In fact, it follows from equation (1) that these symmetries must hold generally since the conformal group includes rotation and inversions (Ramond 1981) that do not alter the scale factors $|w'|$.

Combining equations (4) and (7) allows us to demonstrate the universal vanishing of any critical correlation function $g(w_1, w_2)$ in a circle with free boundaries as one or both points approach the edge. If $|w_1| \to 1 - \varepsilon$ with $|w_2|$ fixed, $g \to \varepsilon^{x_s - x}$; likewise $|w_1| \to 1 - \varepsilon$, $|w_2| \to 1 - \varepsilon'$ results in $g \to (\varepsilon\varepsilon')^{x_s - x} = \varepsilon^{2(x_s - x)}$ if $\varepsilon \propto \varepsilon'$. This result has been found also by Burkhardt and Eisenriegler (1985).

3. Definition of quantities and results for the circle

For probes that couple to the order parameter, the scattering function (structure function) is given by

$$S(\boldsymbol{k}) = \int\int g(w_1, w_2) \exp[\mathrm{i}\boldsymbol{k} \cdot (\boldsymbol{w}_1 - \boldsymbol{w}_2)] \, \mathrm{d}^2 w_1 \, \mathrm{d}^2 w_2. \tag{8}$$

Results for the circle are displayed in figure 1. In performing integrations like those in equation (8), it is generally convenient to make use of the fact that $|w'(z)| = |z'(w)|^{-1}$, which means that the only mapping function necessary is $z = z(w)$ (for the circle, this may easily be obtained by inverting equation (5)). Further details on the numerical procedure used are given below.

Note that figure 1 gives the universal line-shape of $S(\boldsymbol{k})$ for circular geometries. To compare the scattering function for the circle (or any other geometry) with experimental or other theoretical results, several additional quantities must be specified. First, the correlation function used here is not normalised, so there is an undetermined overall multiplicative constant in g and hence $S(\boldsymbol{k})$. This constant also affects the other quantities calculated below, except the correlation length ξ. It depends on the particular system of interest. Secondly, to compare $S(\boldsymbol{k})$ with the experimental scattering intensity (in single-scattering approximation) it must be multiplied by the appropriate cross section. Note, however, that for a given system both these constants need only be determined once. They are independent of the size and shape of the finite regions. Finally, results for regions of the same shape but different size follow by

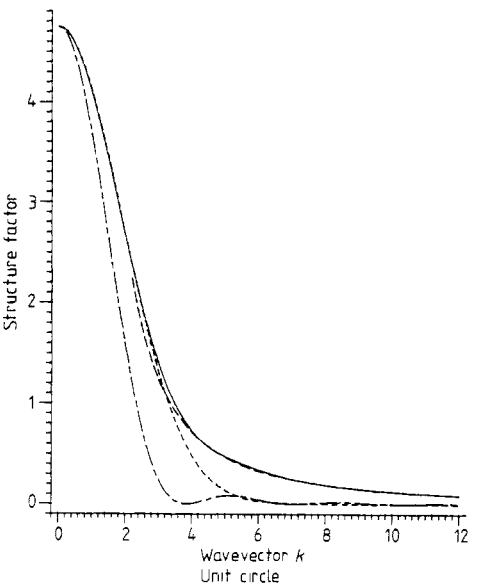

Figure 1. Full curve (——): structure factor $S(\boldsymbol{k})$ (equation (8)) against wavevector k for a circle of radius 1. The line connects 100 data points. Changing the mesh size indicates an absolute error of 0.002 for all k values up to 15. Short broken curve (- - -): Gaussian fit at small k values. Long broken curve (— —): power-law fit for $10 \leq k \leq 15$. A least-squares routine gives $10.04\, k^{-1.908}$, i.e. $\eta_{\mathrm{app}} = 0.09$. Chain curve (· — ·): normalised $S(\boldsymbol{k})$ for perfect order ($g = 1$). Comparison with the full curve illustrates the effects of critical order on the scattering.

ordinary scaling. For instance, if we multiply all lengths by a factor λ, the scattering function obeys

$$S(\boldsymbol{k}, \lambda) = \lambda^{4-0.25} S(\lambda \boldsymbol{k}, 1) \tag{9}$$

where $S(\boldsymbol{k}, 1)$ refers to the 'unit' size of a given shape, e.g. the circle of radius 1. The power $2d = 4$ appears in equation (9) because S is the *total* scattering intensity, and is not normalised to unit area. Further remarks on the application of our results are contained in § 6.

The function $S(k)$ for a circle with free boundaries, illustrated in figure 1, is very accurately represented by a Gaussian for smaller k values, as shown. For intermediate k values, $6 \lesssim k \lesssim 15$, and perhaps higher (numerical problems preclude accurate results for yet larger k—see below), it is extremely well represented by a power law $S \propto 1/k^{2-\eta_{app}}$, where the 'apparent' exponent has the value $\eta_{app} = 0.09 \pm 0.01$. (The error estimate follows from attributing the total error in $S(\pm 0.002)$ to η_{app} and is therefore quite conservative. A least-squares fit error is considerably smaller.) The foregoing result for η_{app} might appear to contradict the 2D Ising model value $\eta = 2x = 0.25$. However, it should be remembered that at $T = T_c$, the thermodynamic limit is not unique. Since the correlation length, which measures the distance over which boundary effects are felt, is proportional to any length n measuring the size of the system, the fraction of the area (or volume) affected does not vanish as $n \to \infty$. Therefore $S(k)$ for free boundaries will in general differ from what is obtained with, e.g., periodic boundaries. It is nonetheless quite interesting that, for the circle, $S(k)$ at T_c has (at least over a certain k range) power-law-like behaviour. Note that this result is by equation (9) independent of the *size* of the circle; no matter how large the radius there will always be a k range in which η_{app} governs the decay of S. At very large k values $S(k)$ will of course go as $1/k^{2-\eta}$ since by equations (1), (2) and (3), $g \to |w_1 - w_2|^{-\eta}$ at small $|w_1 - w_2|$. However, in many cases in experiments or numerical simulations it is difficult to determine $S(k)$ accurately at large k (since S is small) or small k (due to, e.g., forward scattering). Hence, fitting data to a power-law form may lead to 'erroneous' results; i.e. one would be measuring η_{app} rather than η. Notice that for a power-law form this will occur even for an average of $S(k)$ over a range of system sizes. Since η is related to other critical exponents via scaling, this effect could also be important for other quantities. For temperatures close but not exactly equal to T_c, $S(k)$ must cross over to a universal form $1/k^{2-\eta}$ at least for some range of k values. Presumably this will occur, in general, when the finite-system size is of the order of the bulk correlation length (i.e. at fixed scaled temperature). A full analysis would be interesting but is beyond the scope of this paper.

We also examined the Fourier transform of $S(k)$, by calculating $g(w_1, w_2)$ for fixed $r = |w_1 - w_2|$, integrated over all $w_1 + w_2$ values. For small r values ($\lesssim 0.01$) this behaves as $r^{-1/4}$, as it must, but as r increases, the limitation of w_1 and w_2 to a finite region (and the vanishing of g at the boundary) reduces it from this form, so that it vanishes at $r = 2$. This is consistent with the behaviour of $S(k)$ described above.

The (bulk) susceptibility per unit area is simply

$$\chi = S(0)/A \tag{10}$$

where the area $A = \pi$ for the unit circle. For a circle of radius one, we find $\chi = 1.51$.

The specific heat correction term requires separate discussion. The connected energy-energy correlation function in the half-plane with free boundary is (Cardy

1984b)

$$g_E(z_1, z_2) = 4y_1y_2/\{[(x_1-x_2)^2+(y_1-y_2)^2][(x_1-x_2)^2+(y_1+y_2)^2]\}. \tag{11}$$

For this operator the scaling dimension $x = 1$, so that $g_E \sim |z_1 - z_2|^{-2}$ or $|w_1 - w_2|^{-2}$ when the two points approach each other. This means that the total specific heat

$$C = \int g_E(w_1, w_2)\, d^2w_1\, d^2w_2 \tag{12}$$

in any finite region is logarithmically divergent. This behaviour is of course not physical, but results since the conformal theory holds in the continuum limit and the integration in equation (12) includes $|w_1 - w_2|$ values smaller than the lattice constant of any specific system. In computing our results we therefore imposed the condition $|w_1 - w_2| \geq \varepsilon$ (see below for further remarks on this short-distance cut-off). Since g_E is well behaved elsewhere, it follows (see the appendix) that for a circle of radius R

$$C = 2\pi A \ln(R/\varepsilon) + AB(\varepsilon) \tag{13}$$

where A is the area and the specific heat correction term $B(\varepsilon)$ is finite (and intensive). We have calculated $B \equiv B(0)$ by letting $\varepsilon \to 0$ numerically; for the circle we find $B = -8.3$. In this computation, numerical problems associated with the logarithm in equation (13) are encountered in using equation (12) as it stands, since the leading term diverges as ε is decreased. However, if we set $C = C_1 + C_2$, where

$$C_2 \equiv \int |w_1 - w_2|^{-2}\, d^2w_1\, d^2w_2, \tag{14}$$

good convergence is obtained. With this decomposition C_2 includes all of the divergence and part of the term B. It was handled (mainly) analytically as described in the appendix, while C_1 was computed numerically.

Note that the value of the cut-off ε affects both terms (but especially the first!) in the specific heat in equation (13). Therefore it constitutes another quantity that must be determined before comparison with experimental or other theoretical results can be made. This problem does not arise with the spin-spin correlation function because the smaller value of the scaling dimension ($x = \frac{1}{8}$ against 1) precludes short-distance divergences. For the specific heat of a specific system an appropriate value for ε should be of the order of a few lattice spacings.

4. Rectangular (and elliptical) geometries

Results for rectangular-shaped areas were also obtained using the inverse Schwartz-Christoffel transformation (Nehari 1952). The scattering function $S(\boldsymbol{k})$, susceptibility χ and specific heat correction term B were calculated as described above for rectangles of width 2 and various values of the aspect ratio s = length/width. We also determined most of these quantities for an infinite strip ($s = \infty$) by choosing s to exceed the correlation length ξ_y (see below) for $s = \infty$ (the maximum value) and restricting one point in the integration to a strip of width 0.1 centred at the midpoint of the strip. As a check, we performed an independent calculation using the transformation $z = e^{\pi w/2}$, which connects the half-plane and an infinite strip of width 2.

The correlation lengths, defined by

$$\xi_{x,y}^2 = \frac{\int g(w_1 w_2)(\Delta w_{x,y})^2 \, d^2 w_1 \, d^2 w_2}{\int g(w_1 w_2) \, d^2 w_2}, \tag{15}$$

were also computed. For the circle of radius one, we obtained $\xi \equiv (\xi_x^2 + \xi_y^2)^{1/2} = 0.61$.

Equation (15) is appropriate for a finite geometry. Note that ξ_x and ξ_y also provide measures of the inverse linewidths of $S(\boldsymbol{k})$ in the corresponding directions.

For the rectangle, both ξ_x and ξ_y increase with the aspect ratio (figure 2). ξ_x (short direction) approaches its asymptotic ($s = \infty$) value rapidly, being within the expected error by $s = 2$. However, ξ_y (long direction) approaches its infinite strip value in a more complicated fashion. A rapid increase until $s \simeq 5$ is followed by a region in which ξ_y grows slowly with s. Numerical problems (see below) precluded accurate results for $s \gtrsim 10$; however, the $s = \infty$ value clearly exceeds that at $s = 10$, indicating a slow increase of ξ_y for $s > 10$. This may be understood semi-quantitatively as an end effect. Assuming ξ_y takes on its $s = 1$ value in a region of width about one ($s = 1$) correlation length at the ends and its $s = \infty$ value elsewhere gives $\xi_y \simeq \xi_y(1)\ (0.6/s) + \xi_y(\infty)\ (1 - 0.6/s)$ which reproduces the data within the error for $s \gtrsim 5$, but falls above the computed values for smaller s values.

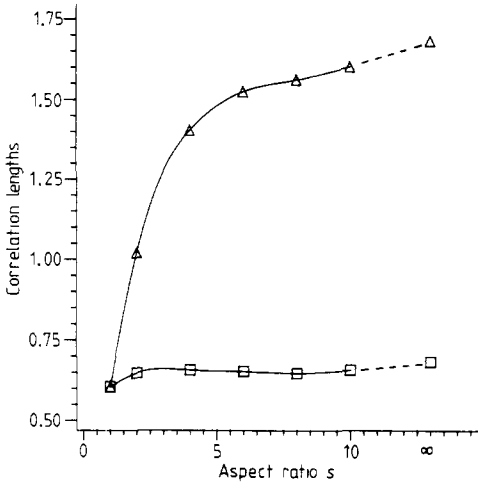

Figure 2. Correlation lengths (equation (15)) for $2 \times 2s$ rectangles. Squares (□) indicate ξ_x, the short direction, triangles (△) ξ_y, the long direction. Here and in figures 3-6 full lines are spline fits. From changing the mesh size, we estimate an error within the size of the symbols. For a rectangle with perfect order ($g = 1$) one finds $\xi_x = \sqrt{2/3} = 0.816$, $\xi_y = \sqrt{2/3}\, s = 0.816\, s$. For a circle of unit radius we found $\xi \equiv (\xi_x^2 + \xi_y^2)^{1/2} = 0.61$. Writing $\xi = \xi_0 A^{1/2}$, where A is the area, gives $\xi_0 = 0.34$ for the circle and 0.43 for the square.

For the infinite strip, one can define ξ_y as a moment (equation (15)) or via the asymptotic behaviour of the correlation function, $g \to e^{-|y|/\xi}$ as $|y| \to \infty$. To compare these two definitions it is useful to introduce a factor of $\frac{1}{2}$ on the RHS of equation (15). With this slightly altered definition, the two values of ξ_y will coincide exactly for the case of an exponential correlation function $g(x_1, x_2, y) = e^{-|y|/\xi}$. Making this change, the moment values of ξ_y for the infinite strip is 1.17. This is within 10% of its asymptotic value (Cardy 1984a) $\xi_y = 2n/\pi\eta_{\|} = n/\pi x_s = 1.27$, using the strip width $n = 2$ and $x_s = \frac{1}{2}$ for the Ising model. The moment value is also less than the asymptotic value (2.55)

for the *periodic* boundary case (Kleban and Akinci 1983a), as one would expect. Also, for the finite rectangle, ξ_y grows similarly with s for either boundary condition. In particular, if one removes end effects from the free boundary values the two cases are very close to each other for $1 \lesssim s \lesssim 5$, with the (approximate) periodic values rising faster for $s \gtrsim 5$. A change in ξ_y against s near $s = 5$ is observed for the subtracted values. We will see that a similar effect also occurs in the susceptibility and specific heat correction term.

The behaviour of the scattering function $S(\boldsymbol{k})$ for various s values is shown in figures 3 and 4. The linewidths as a function of s clearly reflect the trends exhibited by the correlation lengths, discussed above. For $s = 1$, a power law fits the decay of S over the range $2 \leq k_{x,y} \leq 8$ reasonably well with a power consistent with that found for the circle ($\eta_{\text{app}} = 0.09$). For $s = 2$ and ∞, $S(k_x)$ for $2.5 \leq k_x \leq 10$ may be represented by $\eta = 0$. When $s = 2$, $S(k_y)$ over this range resembles the square ($s = 1$) case. It is too 'noisy' for a reasonable fit at $s = \infty$, where a power-law fit is not distinguishable from an exponential. Generally, for larger s values a power-law fit becomes less accurate. It is not clear whether this is due to errors in the computation or the inherent behaviour of S.

The bulk susceptibility (per unit area) against s is shown in figure 5. According to the results of Kleban and Akinci (1983a, b) the shape dependence of the finite-size corrections to the specific heat near T_c for an Ising model with *periodic* boundary conditions in a rectangular region may be understood in terms of a 1D Ising array of domain walls. At $T = T_c$, the number of domain walls in this array is independent of

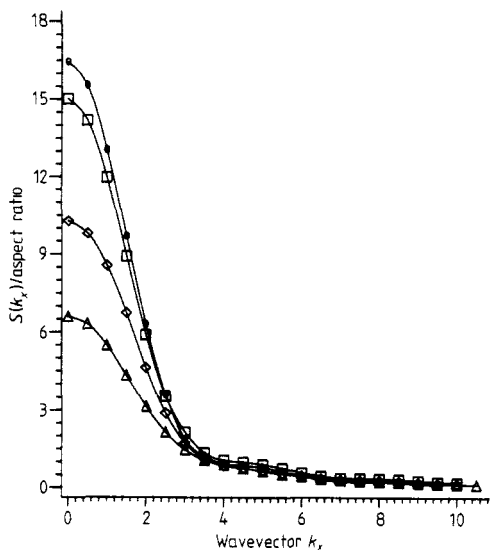

Figure 3. Scattering function $S(k_x)/s$ against wavevector k_x (short direction) with $k_y = 0$ for $2 \times 2s$ rectangles. Triangles (△): $s = 1$, diamonds (◇): $s = 2$, squares (□): $s = 6$, open circles (○): $s = \infty$. Here and in figures 4 and 5 the square estimates the error for all curves. The hump near $k = 5$ would probably disappear if the mesh size were decreased—similar effects were seen in the circular geometry.

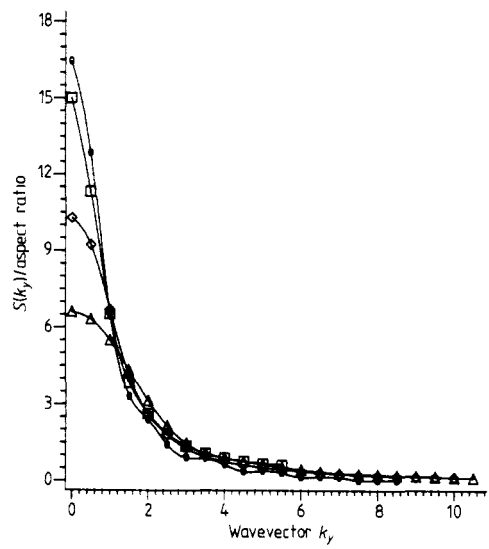

Figure 4. Same as figure 3, with k_x replaced by k_y (long direction). The oscillations for $s = \infty$ are within expected error; we believe this structure is a numerical effect. The convergence to $s = \infty$ for figure 3 (k_x) and here (k_y) at a given wavevector in the large k region ($k \gtrsim 3$) mimics the behaviour of the corresponding correlation length against s shown in figure 2.

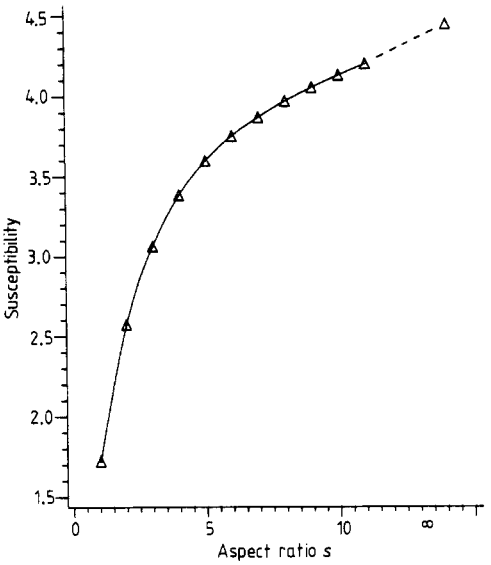

Figure 5. Bulk susceptibility χ (equation (10)) against aspect ratio for the rectangle. For a circle of radius one, we found $\chi = 1.51$. The s dependence of this quantity (and the specific heat correction term, figure 6) is discussed in terms of a 1D Ising array of domain walls and edge effects in the text.

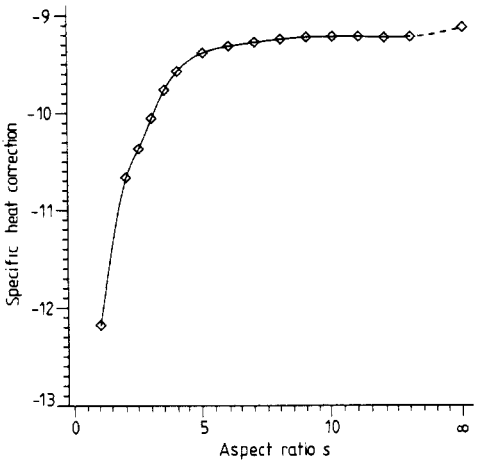

Figure 6. Specific heat correction term B (equation (13)), with R replaced by the width $n = 2$ against aspect ratio s for the rectangle. For the circle of radius 1, using equation (13) we find $B = -8.3$ whereas for the square $B = -12.1$. Note, however, that if we write $C/A = 2\pi \ln(A^{1/2}/\varepsilon) - B'$, so as to compare figures of equal area, $B' = -11.9$ for the circle and -12.1 for the square. The percentage error in the results given in this figure is probably larger than in the other cases reported.

size but increases with the shape parameter s. Thus the s dependence of the 2D quantity is given by the length dependence of the corresponding quantity in a 1D Ising model. Such an array is also expected to be present with free boundaries. Since the susceptibility per spin of the 1D Ising model with free ends grows with the number of spins, the array may be expected to contribute a term to χ that increases with s at large s. In addition to this array, one expects a contribution to χ from end and edge effects. For an $(m \times n)$ rectangle the total number of spins involved should be proportional to $n\xi_m + m\xi_n$. As can be seen from figure 2, this results in a number of spins per unit area that decreases with s, approaching a constant as $s \to \infty$. Thus if their contribution to χ does not dominate the domain wall contribution, the net effect is a term that grows with s, as observed.

If one subtracts off an assumed end contribution to χ as was done for ξ_y above, the result lies above the data for $s \geq 5$ (and for lower s values as well), suggesting that domain wall and edge contributions to χ have not yet reached their asymptotic values at $s = 5$. Unfortunately it appears difficult to make these interpretations more quantitative since the relative magnitude of various quantities is unknown and there could be an influence of the edge spins on the domain walls.

Results for the specific heat correction term $B(0)$ as defined in equation (13), but with R replaced by $n = 2$ against the shape $s = m/n = 2s/2$, are shown in figure 6. Note that B behaves very differently than for the 2D Ising model with *periodic* boundaries

(Ferdinand and Fisher 1969) where it is always positive, and shows a maximum as s increases. This latter behaviour is due to a 1D array of domain walls. In the present case, the 1D array with free ends should make a contribution to B that is negative but decreases in magnitude with s, in agreement with the overall trend exhibited in figure 6. This is expected since there is no shift in the specific heat maximum for a 1D Ising model with free ends. In addition, edge spins should also be considered. For the 2D Ising model the edge specific heat per spin near T_c is negative for a long strip (McCoy and Wu 1967, Binder 1983). As explained above, the number of edge spins per unit area decreases to a constant as s grows. Thus both terms should contribute similarly to B.

Attempts to make this picture more quantitative have not been successful. One problem is that the dependence of the domain wall energy on (scaled) temperature near T_c is not known for free boundaries—using the periodic boundary values (Kleban and Akinci 1983a) gives a contribution to B that is too small by about an order of magnitude and has the wrong sign.

Subtracting end effects from the computed values of B as was done for ξ_y and x gives a result that agrees within the error for $s \gtrsim 5$, suggesting that domain wall and edge contributions to B no longer vary with s in this range.

It is also interesting to compare the value of B at $s = \infty$ with the exact result of Au-Yang and Fisher (1975) who find

$$C/k_B = A_0 \ln n + B_\infty \tag{16}$$

for an $(n \times \infty)$ simple Ising model, where C is the specific heat per spin and $A_0 = 0.494\,5386\ldots$, $B_\infty = -0.312\,5538\ldots$. As explained above, a direct comparison of equations (13) and (16) requires specification of both an overall multiplicative constant and the short-distance cut-off ε, since neither quantity is determined by the conformal theory. If we take $\varepsilon = 1$, we find that the B value exhibited in figure 6 is too negative by a factor of 2.3. The correct ratio of A_0/B_∞ is obtained if we take $\varepsilon = 0.44$. This indicates that (at least on average) g_w is underestimated by the conformal theory or that short-range corrections (which are of the same order as B) are important. The latter possibility could arise from the relatively large critical dimension ($x = 1$) of the energy operator which emphasises short-range behaviour.

We have also calculated for elliptical shapes by making use of the transformation from an ellipse to the circle of unit radius given by Nehari (1952). This required considerable computation time, so a few results were obtained for $S(\boldsymbol{k})$ only. They are rather similar to the rectangular case.

5. Application to experimental and model systems

We now consider further the relevance of our results to experimental and model systems. First we emphasise that the conformal mapping technique is valid only at T_c. This makes comparison with existing analytic and numerical results difficult, since there are very little data valid exactly at T_c. On the other hand it illustrates the value of this method in extending what is known. For experimental systems, the problem of determining T_c is posed. A general method for doing this is described by Bartelt *et al* (1985). For T near T_c (when one is in the critical region), the appropriate variable is the scaled temperature $\tau = L/\xi_\infty$, where L is a typical dimension and ξ_∞ the infinite system correlation length. Now, taken as functions of scaled temperatures (Barber

1983, Kleban 1984), one does not in general expect finite-size quantities to vary rapidly near a second-order transition. Hence results valid at T_c should be useful in understanding behaviour in the rest of the critical region.

Secondly, the conformal results are only valid in the continuum limit, as mentioned in the introduction. This implies that the conformal results for a correlation function break down at short distances: here, when the two points are too close together or one or both of them is too close to the edge. Thus, for a given system, one should in principle cut off the integrals in $S(\boldsymbol{k})$, for instance, to account for this. The cut-offs to be taken are not universal, and cannot be determined without further knowledge about the specific system. However, for the spin–spin correlation function, the integrals computed here depend only very weakly on these values. For the energy–energy case, the short-distance cut-off does matter, as described above. One might worry about the effects of these corrections if the system is scaled up in size. We have not attempted to address this concern generally. However, we note that by general scaling arguments the distance over which these corrections are felt cannot grow faster than the correlation length, which is always proportional to a typical dimension, hence the relative area influenced will not increase. Also, in a more general sense, the success of the phenomenological renormalisation group in predicting bulk quantities from numerical results for very small systems gives confidence in the value of results from conformal theory.

Furthermore, this short-distance cut-off implies that conformal results for $S(\boldsymbol{k})$ apply only for $k \lesssim 1/a$, where a is a lattice spacing. Recent Monte Carlo simulations (Bartelt and Einstein 1986) for the simple Ising model on square lattices of sizes up to 60×60 lattice spacings show excellent agreement (within our numerical errors) with the conformal results for $k \leq \pi/2a$, i.e. k values from the Brillouin zone centre to halfway to the zone edge.

Since conformal invariance includes rotational invariance (Ramond 1981), our results are restricted to systems with isotropic fixed point Hamiltonians (Cardy 1984b). This means, e.g., that they apply to Ising transitions on lattices with a square unit mesh, but (in general) not to rectangular meshes.

Another potential problem for real systems has been pointed out by Burkhardt and Eisenriegler (1985). As mentioned above, the scaled temperature is defined by $\tau = L/\xi_\infty$. At T_c, where conformal results are valid, $\tau = 0$. However, if L is large, temperature uncertainties may induce large values of τ, giving rise to errors. This certainly can be a problem; however, it should be mentioned that the evidence (Ferdinand and Fisher 1969, Binder 1983, Barber 1983) indicates that many quantities are *not* strong functions of τ near $\tau = 0$, mitigating this effect.

In applying the results of this work to real surface systems the restriction to free boundary conditions must also be remembered. This implies that there is no ordering field at the edge of the region in question. For adsorption systems, one generally expects the edge to consist of random defects or randomly arranged step edges. For strong (or weak) adsorption sites, such as one might encounter at the terrace edges on a stepped surface (Kleban 1981, Kleban and Flagg 1981), there are several possibilities. If the edge sites prejudice the adsorbate into one ordered state (e.g. for strong sites and (1×1) order) the results given here do not apply. If, on the other hand, edge effects favour an ordering of different symmetry from that characterising the phase transition, or if they favour no order at all, the order near the boundary will be reduced, as for free boundary conditions. To the extent that these effects are similar, our calculations are applicable. If there are, in particular, randomly arranged strong

and weak sites at the edge, a model with quenched random fields at the boundaries is probably appropriate. However, we are not aware of any general treatment of this problem so it is not clear how it relates to the free boundary case. If one has an array of uniformly stepped terraces on a stepped surface, correlated one-dimensional random fields could arise, as has been pointed out elsewhere (Clements and Kleban 1984). Similar remarks apply for phase transitions involving surface reconstruction.

The scattering function $S(\boldsymbol{k})$ defined by equation (8) is ideal in that it applies to instruments with infinite coherence length (spatial resolution). To model the effects of a finite instrument coherence L_I one generally convolutes $S(\boldsymbol{k})$ with a Gaussian function chosen to model the instrumental parameters. In the limit that the dimension n of the ordered region exceeds L_I, the scattering function will no longer have the shape computed here. Its magnitude will then be determined by *local* correlations the expectation values of which are energy-like. Its shape will be determined by the resolution and therefore will vary on the scale of $1/L_I$ rather than $1/n$.

Another point of interest for experimental studies is that the conformal method allows the possibility of including the effects of critical order in finite regions on multiple scattering at a second-order phase transition. Multiple scattering is important for many commonly used probes, e.g. low energy electron diffraction (LEED). By the local algebra hypothesis all correlations at T_c can be expressed as linear combinations of a certain basis set. For the Ising case, this consists of the spin-spin and energy-energy correlation functions.

Finally we remark that the projective transformation of the surface of a sphere onto the infinite plane is also conformal. We hope to explore the consequences of this elsewhere.

6. Computational details

We now give some technical details of the computations performed. We used standard Gaussian integration routines. For the circle map, it was possible to express the integrand as a function of three variables, with $(48)^3 \simeq 111\,000$ function evaluations employed and a mesh size of $1/48$. For the rectangle and ellipse, the problem is four-dimensional, with no such reduction possible. Results reported here employed either $(2^3)^4 \simeq 65\,536$ or $(2^4)^4 \simeq 10^6$ evaluations, requiring substantial amounts of computer time. Expected errors in our results are given in the figures. Note that with $2^4 = 16$ points along each dimension, the long side of a $2 \times 2s$ rectangle has a mesh size $\delta y = s/8$. For the correlation lengths encountered here, this implies problems in calculating χ or the correlation lengths themselves for $s \gtrsim 14$. For $S(\boldsymbol{k})$, assuming $\delta \gtrsim \lambda/4$ as a criterion similarly leads to $k_y \gtrsim 12/s$, $k_x \gtrsim 12$.

Considerable care was taken with the computer programs employed, in part because of the paucity of previous results for comparison. Part of the circle and infinite strip results were obtained with independently written programs. Several non-trivial checks on the results were used to help ensure accuracy.

Acknowledgments

We would like to acknowledge several useful and stimulating conversations with J Cardy, whose patient explanations greatly aided our understanding of the conformal

theory. We also thank K Penson for bringing the work of Burkhardt and Eisenriegler (1985) to our attention, and A N Berker for a useful remark.

Appendix

In this appendix we derive the expression for the specific heat (equation (13)) and a formula for the term

$$C_2 = \int |w_1 - w_2|^{-2} \, \mathrm{d}^2 w_1 \, \mathrm{d}^2 w_2. \tag{A1}$$

These results are necessary for the integration of the energy-energy correlation function, to obtain the specific heat correction term B (see equation (13)). First we note that the integrand in (A1) must be replaced by zero for $|w_1 - w_2| < \varepsilon$, to avoid divergence. This short-distance cut-off is related to the lattice spacing (see text). With this restriction in equation (A1), two applications of Gauss's theorem result in

$$C_2 = -\tfrac{1}{2} \int\int \mathbf{d}\boldsymbol{l}_1 \cdot \mathbf{d}\boldsymbol{l}_2 \theta(|w_1 - w_2| - \varepsilon) \ln^2 \frac{|w_1 - w_2|}{\varepsilon}. \tag{A2}$$

In (A2), $\boldsymbol{l}_1$ and $\boldsymbol{l}_2$ are outward directed vectors, θ the unit step function, and the integration is around the circumference of the region of interest. For $\varepsilon \to 0$, it is easy to see that removing the θ function in (A2) gives rise to an error less in magnitude than

$$\lim_{\alpha \to 0} \int \mathrm{d}l_1 \int_{\alpha}^{\varepsilon} \ln^2\left(\frac{x}{\varepsilon}\right) \mathrm{d}x = \lim_{\alpha \to 0} \varepsilon \int \mathrm{d}l_1 \int_{\alpha/\varepsilon}^{1} \ln^2 z \, \mathrm{d}z \tag{A3}$$

$$= 2\varepsilon D$$

where D is the circumference. Hence, for small ε,

$$C_2 = -\tfrac{1}{2} \int\int \mathbf{d}\boldsymbol{l}_1 \cdot \mathbf{d}\boldsymbol{l}_2 \ln^2(|w_1 - w_2|/\varepsilon). \tag{A4}$$

Introducing the (arbitrary) factor L in the logarithm and noting that a constant integrand in (A4) gives zero leads to

$$C_2 = \int\int \mathbf{d}\boldsymbol{l}_1 \cdot \mathbf{d}\boldsymbol{l}_2 \ln \frac{|w_1 - w_2|}{L} \ln \frac{L}{\varepsilon} - \tfrac{1}{2} \int\int \mathbf{d}\boldsymbol{l}_1 \cdot \mathbf{d}\boldsymbol{l}_2 \ln^2 \frac{|w_1 - w_2|}{L}. \tag{A5}$$

Applying Gauss's theorem to the first term then gives

$$C_2 = 2A\pi \ln(L/\varepsilon) + K \tag{A6}$$

where A is the area of the region integrated over and

$$K = -\tfrac{1}{2} \int\int \mathbf{d}\boldsymbol{l}_1 \cdot \mathbf{d}\boldsymbol{l}_2 \ln^2 \frac{|w_1 - w_2|}{L}. \tag{A7}$$

The first term in (A6) contains the logarithmic divergence of the Ising model specific heat. The second term is proportional to L^2, so that for ordinary regions it gives a contribution to the (extensive) specific heat correction term AB.

For a circle of radius $R = 1$, we can set $L = R = 1$. Then

$$K = -\tfrac{1}{2}2\pi \int_0^{2\pi} d\theta \cos\theta \ln^2(2 \sin \tfrac{1}{2}\theta). \tag{A8}$$

If we let $\phi \equiv \theta/2$ and integrate by parts, we find

$$K = 2\pi \int_0^{\pi} (1 + \cos 2\phi) \ln(2 \sin \phi)\, d\phi.$$

Integrating by parts once again gives

$$K = -\pi^2 \tag{A9}$$

where use has been made of the integral

$$\int_0^{\pi/2} \ln(\sin \phi)\, d\phi = -\tfrac{1}{2}\pi \ln 2. \tag{A10}$$

The result (A9) gives part of the specific heat correction term $B(0)$ for the circle in equation (13).

For an $m \times n$ rectangle, for $L = 1$, K reduces by elementary methods to

$$K = K(m, n) + K(n, m) \tag{A11}$$

where

$$K(m, n) = \tfrac{1}{2} \int_0^{m} (m - y) \ln^2(y^2 + n^2)\, dy - m^2(\ln^2 m - 3 \ln m + \tfrac{7}{2}). \tag{A12}$$

The integral on the RHS of (A12) apparently cannot be evaluated analytically. The results in figure 6 include a contribution from equations (A11) and (A12) for $n = 2$, $m = 2s$. Dividing by the area $A = mn = n^2 s$, one finds

$$K/A = (1/4s)[K(2s, 2) + K(2, 2s)] \tag{A13}$$

for the part of B arising from C_2. In the limit $s \to \infty$, this reduces to

$$K/A = \tfrac{1}{2} \int_0^{\infty} [\ln^2(x^2 + 1) - \ln^2 x^2]\, dx$$
$$= 2\pi(\ln 2 - 1).$$

References

Au-Yang H and Fisher M E 1975 *Phys. Rev.* B **11** 3469

Barber M N 1983 *Phase Transitions and Critical Phenomena* vol 8, ed C Domb and J L Lebowitz (London: Academic) pp 146-268

Bartelt N and Einstein T L 1986 *J. Phys. A: Math. Gen.* **19** to be published

Bartelt N, Einstein T L and Roelofs L 1985 *Surf. Sci.* **149** L47

Belavin A A, Polyakov A M and Zamolodchikov A B 1984a *Nucl. Phys.* B **241** 333

—— 1984b *J. Stat. Phys.* **34** 763

Binder K 1983 *Phase Transitions and Critical Phenomena* vol 8, ed C Domb and J L Lebowitz (London: Academic) pp 2-145

Burkhardt T and Eisenriegler E 1985 *J. Phys. A: Math. Gen.* **18** L83

Cardy J L 1984a *J. Phys. A: Math. Gen.* **17** L385
—— 1984b *Nucl. Phys.* B **240** (FS12) 514
Clements B E and Kleban P 1984 *Surf. Sci.* **138** 211
Dotsenko V S 1984a *Nucl. Phys.* B **235** (FS11) 54
—— 1984b *J. Stat. Phys.* **34** 781
Ferdinand A E and Fisher M E 1969 *Phys. Rev.* **185** 832
Friedan D, Qiu Z and Shenker S H 1984 *Phys. Rev. Lett.* **52** 1575
Kleban P 1981 *Surf. Sci.* **103** 542
—— 1984 *Chemistry and Physics of Solid Surfaces V* ed R Vanselow and R Howe (Berlin: Springer) pp 339–64
Kleban P and Akinci G 1983a *Phys. Rev.* **28** 1466
—— 1983b *Phys. Rev. Lett.* **51** 1058
Kleban P and Flagg R 1981 *Surf. Sci.* **103** 552
McCoy B and Wu T T 1967 *Phys. Rev.* **162** 436
Nehari Z 1952 *Conformal Mapping* (New York: McGraw-Hill)
Polyakov A M 1970 *Zh. Eksp. Teor. Fiz. Pis. Red.* **12** 538 (*JETP Lett.* **12** 381)
—— 1974 *Zh. Eksp. Teor. Fiz. Pis. Red.* **66** 23 (*JETP Lett.* **39** 10)
Ramond P 1981 *Field Theory* (Reading, MA: Benjamin)
Tracy C A and McCoy B M 1975 *Phys. Rev.* B **12** 368
Wegner F 1976 *Phase Transitions and Critical Phenomena* vol 6, ed C Domb and M S Green (London: Academic)